Journal of Zhejiang University SCIENCE A
ISSN 1673-565X (Print); ISSN 1862-1775 (Online)
www.zju.edu.cn/jzus; www.springerlink.com
E-mail: jzus@zju.edu.cn

# Geochemical characteristics of the fluid inclusions in the Gangxi Fault Belt, Huanghua Depression, Bohai Bay Basin, China*

DING Wei-wei†[1], DAI Jin-xing[2], CHU Feng-you[1], HAN Xi-qiu[1]

([1]*Key Laboratory of Submarine Geoscience, the State Oceanic Administration, Hangzhou 310012, China*)

([2]*Department of Earth Science, Zhejiang University, Hangzhou 310027, China*)

†E-mail: wwdingsio@yahoo.com.cn

Received Oct. 20, 2006; revision accepted Nov. 21, 2006

**Abstract**: We studied the geochemical characteristics of the fluid inclusions in the Ordovician carbonates and the Oligocene Shahejie Formation sandstones from 15 wells in the Gangxi Fault Belt, Huanghua Depression. The fluid inclusions are all secondary with gas/liquid ratio of 5%~10%. Base on Raman they are mainly composed of $H_2O$, $CO_2$ and $CH_4$. The homogenization temperatures, combined with burial and geothermal history of the host rock, indicate that the fluid flows in the Shahejie Formation and the Ordovician carbonates were trapped in Neocene. Using a VG5400 mass spectrometer, the helium isotopic compositions were analyzed. Interpretation of results suggested a significant amount of mantle-derived helium mainly accumulating in the intersections of the NWW trending Xuzhuangzi and NE trending Gangxi faults. The maturity of hydrocarbon decreases from the intersection to the outside pointing out that the fluid related to the NWW trending Xuzhuangzi and NE trending Gangxi faults. These factors implied the fluid inclusions have a close relationship to the local tectonic setting. Gangxi Fault Belt experienced intensive Neo-tectonic activities in Cenozoic. Widespread faulted-depressions and strong volcanic eruptions manifested its tectonic status of extensional stress field. Mantle uplift caused the movement of magma that carried mantle-derived gases and deep heat flows, the deep-rooted tension faults provided the passages for the gases and heat flows to shallow crust levels.

**Key words**: Gangxi Fault Belt, Fluid inclusion, Composition, Mantle-derived, Maturity, Local tectonic setting
**doi**:10.1631/jzus.2007.A1011 **Document code**: A **CLC number**: P58; P59

## INTRODUCTION

After diagenesis fluid inclusions will develop in the crannies of the solid rocks with the influence of the tectonic action, or hydrotherm. By studying fluid inclusions we can gain pristine geochemical information about the compositions (Pang *et al*., 1998; Aplin *et al*., 1999; Moore *et al*., 2001), past migration processes and pressure-temperature conditions when the fluid was trapped (England *et al*., 1987; Thiéry *et al*., 2002). In recent years fluid inclusions have been applied to the study of natural gas source origin and tracing (Dai *et al*., 1995; Xu *et al*., 1998; Dallai *et al*., 2005), oil and gas reservoirs' evolution and filling history (Thiéry *et al*., 2002; Feely and Parnell, 2003; Xiao *et al*., 2002; Cao *et al*., 2006), interaction of the crust with the mantle (Stuart *et al*., 1995; Rocholl *et al*., 1996; Valbracht *et al*., 1996; Bach *et al*., 1999; Hoke *et al*., 2000; Doğan *et al*., 2006), ore deposits (Burnard *et al*., 1999; Hu *et al*., 2004; Kendrick *et al*., 2001), tectonics (Oxburgh and O'Nions, 1987; Tao *et al*., 1997; Xu, 1997; Graupner *et al*., 2006), geothermal flow (Polyak *et al*., 1985; Muramatsu *et al*., 2006), etc. In this paper we aim to study the geochemical characteristics of the fluid inclusions of Ordovician carbonates and Oligocene Shahejie Formation's sandstones, Gangxi Fault Belt, Huanghua Depression, Bohai Bay Basin, China, to reveal their origin, trapping time, formation mechanism and geological significances.

* Project supported by the Key Laboratory of Marginal Sea Geology, South China Sea Institute of Oceanology, Chinese Academy of Sciences (No. MSGL0609) and the Chinese Academy of Sciences (No. KZCX2-209)

## GEOLOGICAL SETTING AND SAMPLING

Huanghua Depression lies in the middle of the Bohai Bay Basin. It is a faulted-depression developed in Cenozoic. It has widespread NE-NEE direction rift systems and strong magmatic activities (Fig.1). The Gangxi Fault Belt is the most active area in the Huanghua Depression. The activity started in the Indo-China period (250~205 Ma), and continued during the Yanshan period (205~±60 Ma), with basalts erupted along the belt (ECPGDO, 1991). In the Cenozoic the belt was in extensional stress field and experienced strong extensional activities. Not only rich hydrocarbon reservoirs, but also natural gas accumulations, such as the Zhaizhuangzi $CO_2$ pool, were discovered here. The $CO_2$ content in Well Gang 151 of this pool is up to 98.61% (Dai *et al*., 1994). Fifteen core samples of the Ordovician carbonates and the Oligocene Shahejie Formation's sandstones were collected to study the geochemical characteristics of the fluid inclusions in the study area.

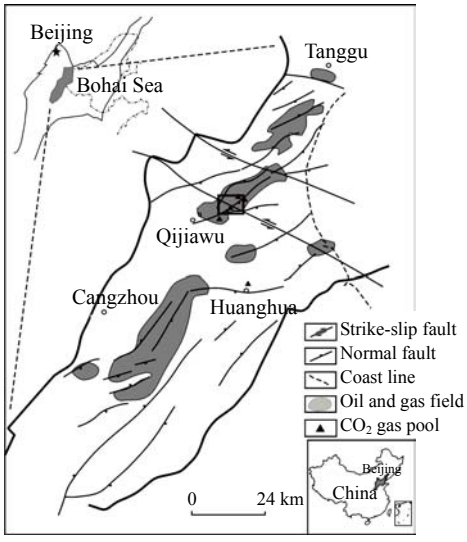


**Fig.1 Geological sketch map of the Huanghua Depression and the distribution of the oil and gas fields and $CO_2$ gas pools. The pane shows the studied area**

## ANALYTICAL METHODS

### Chemical composition of fluid inclusions

Laser Raman micro-spectrometry (LRM) was applied to analyze the chemical compositions of single fluid inclusions. An optical microscope was equipped with high numerical aperture objectives to focus the exciting radiation (the laser beam onto the sample). The experimental conditions with this instrument are $Ar^+$ laser with wavelength of 514.5 nm, energy of 600 μW, double color filter of 450 μm, color of 9.2 $cm^{-1}$/mm, high voltage of 1530 V, room temperature of 23 °C with 65% relative moisture. Each composition was detected by symmetric stretching vibration around the following parameters: $CO_2$ (1387 $cm^{-1}$), $H_2O$ (3410~3705 $cm^{-1}$), $N_2$ (2330 $cm^{-1}$), $H_2S$ (2609 $cm^{-1}$), $CH_4$ (2910~2915 $cm^{-1}$), $SO_2$ (1150 $cm^{-1}$), $H_2$ (4157 $cm^{-1}$) and CO (2144 $cm^{-1}$).

### Helium isotope composition of fluid inclusions

The fluids in the inclusions were extracted by Vacuum Electric Magnetic Breaker in the State Key Laboratory of Gas-Geochemistry, Lanzhou Institute of Geology, Chinese Academy of Sciences. The helium isotopes in the inclusions were measured on a VG5400 mass spectrometer. The selected core samples were crushed to 24~60 mesh and baked at ca. 400 °C on-line with ultra vacuum system for over 24 h. The vacuum pressure was less than $1\times10^{-2}$ Pa in order to desorb gases from the rock surface. The gases released from the inclusions then passed through a cold trap (−80 °C) to remove water before entering a VG5400 mass spectrometer to measure the total amount and concentration of gas compositions (Sun and Chen, 1998).

## RESULTS

### Characteristics of the fluid inclusions

Thin sections under microscope show that all of the fluid inclusions are secondary (Table 1). The fluid inclusions in the Ordovician carbonates mainly occur in the cleavage crack and calcite vein of the sparry calcite. They are straw yellow, yellow, brown or dark brown, and are two-phase aqueous fluid inclusions containing a NaCl (±$CaCl_2$) brine and vapour bubbles. The gas/liquid ratios are generally 5%. Some can reach to 10%. The majority of the clustered inclusions typically exhibit circle or ellipse shapes, 2~3 μm~4~5 μm in size (Fig.2). The fluid inclusions of sandstones

**Table 1 Characteristics of the inclusions in Gangxi Fault Belt, Huanghua Depression**

| Well | Strata | Depth (m) | Lithology | Inclusions No. | Characteristics of inclusion | | | | | | | |
|---|---|---|---|---|---|---|---|---|---|---|---|---|
| | | | | | Host mineral | Occurrence | Size (μm) | Vapor/liquid ratio (%) | Colour | Facies | Origin | $T_h$ (°C) (range/average) |
| F29 | $Es_1$ | 3014.29 | Sandstone | 6 | Quartz | Crack | 2~4 | 5~10 | Straw yellow | Organic gas+brine | Secondary | (147.8~162.5) /157.4 |
| F14 | $Es_1$ | 3084.23 | Sandstone | 6 | Quartz | Crack | 2~4 | 2~5 | Straw yellow | Organic gas+brine | Secondary | (110.5~140.2) /123.9 |
| S10 | $Es_2$ | 2343.46 | Sandstone | 4 | Quartz | Crack | 2~5 | 5~10 | Hazel, brown | Organic gas+brine | Secondary | (126.2~144.5) /135.9 |
| T16 | $Es_3$ | 3442.57 | Sandstone | 6 | Quartz | Crack | 2~5 | 5~10 | Straw yellow, hazel | Organic gas+brine | Secondary | (142.3~155.6) /148.3 |
| Q85 | $Es_3$ | 3024.45 | Sandstone | 4 | Quartz | Crack | 2~5 | 2~5 | Straw yellow, yellow | Organic gas+brine | Secondary | (158.7~173.2) /168.1 |
| T9 | O | 2996.27 | Carbonate | 4 | Sparry calcite | Cleavage | 2~8 | 5~10 | Yellow, hazel | Organic gas+brine | Secondary | (160.5~176.3) /168.9 |
| F4 | O | 2214.09 | Carbonate | 6 | Calcite | Crack | 2~8 | 5~10 | Straw yellow, hazel | Organic gas+brine | Secondary | (145.6~178.5) /162.2 |
| T12 | O | 1980.00 | Carbonate | 5 | Sparry calcite | Cleavage | 2~5 | 5~10 | Straw yellow | Organic gas+brine | Secondary | (165.8~178.5) /170.5 |
| T13 | O | 2065.00 | Carbonate | 4 | Calcite | Crack | 2~4 | 2~5 | Straw yellow, hazel | Organic gas+brine | Secondary | (158.2~172.3) /165.4 |
| T14 | O | 3043.00 | Carbonate | 5 | Calcite | Crack | 2~5 | 2~5 | Hazel, brown | Organic gas+brine | Secondary | (147.3~168.3) /155.8 |
| T15 | O | 2618.98 | Carbonate | 2 | Calcite | Crack | 2~8 | 10 | Hazel, puce | Organic gas+brine | Secondary | (160.3~166.4) /163.4 |

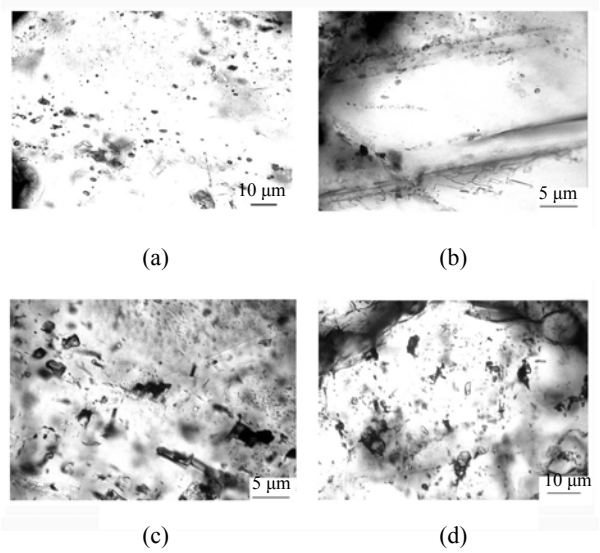


**Fig.2 Typical inclusions. (a) Well F29. The inclusions distributed clusters along microfractures of quartz; (b) Well T12. The inclusions occur in the cleavage crack of the sparry calcite; (c) Well T13. The inclusions occur in the crossing calcite vein of the sparry calcite; (d) Well T15. The inclusions occur in the calcite**

in the Shahejie Formation mostly occur in the microfractures. They are also secondary. Quartz largen occurs in the sample of Well S10, and inclusions are observed occasionally in it. The colors are generally straw yellow. The fluid inclusions are also two-phase inclusions with gas/liquid ratios being 5%~10%. The sizes are mostly 2~4 μm.

### Homogenization temperature ($T_h$)

The THMS-G600 micro-stage of Linkcam Company was used to measure the hemogenization temperature of fluid inclusions. Heating rates of 5 °C/min were used. These were reduced to 1 °C/min close to transition points in order to define precisely the temperatures on which phase changes occur. The same rates were used for heat-cool-cycling. The temperature control precision is ±0.1 °C. Fifty two inclusions were measured, among them were twenty six inclusions from the Ordovician carbonates, six inclusions from the first member of the Shahejie Formation ($Es_1$), four inclusions from the second

member of the Shahejie Formation ($Es_2$), sixteen inclusions from the third member of the Shahejie Formation ($Es_3$) (Table 1). The $T_h$ of the Ordovician carbonates' inclusions is between 145.6 °C and 178.5 °C, with a mean from 160 °C to 170 °C. The $T_h$ of the inclusions in $Es_1$ ranges from 102.3 °C to 140.2 °C, average of 123.9 °C. The $T_h$ of the inclusions in $Es_2$ ranges from 126.2 °C to 144.5 °C, average of 136.1 °C. The $T_h$ of the inclusions in $Es_3$ ranges from 142.3 °C to 173.2 °C. The average $T_h$ differs in different wells. The average in Well F29 is 157.4 °C, in Well T16 is 148.3 °C and in Well Q85 is 168.1 °C.

## Gaseous composition

The gaseous compositions of the fluid inclusions in terms of molar proportions are listed in Table 2. Typical Raman spectra are given in Fig.3. The principal composition is $H_2O$, which ranges from 42.47 mol% to 82.93 mol%. $CO_2$ and $CH_4$ make up the bulk of the remaining. LRM analyses yielded $CO_2$ concentrations of 1.25~34.68 mol% whereas the $CH_4$ concentrations range from 0.47 to 9.54 mol%. No $CO_2$ was detected in Well F29. Hydrocarbon compounds other than $CH_4$ are present in most of the samples. Data were obtained on the light hydrocarbons ranging from ethyne ($C_2H_2$) to toluene ($C_6H_6$). The abundances of the hydrocarbons are variable. The concentration of $C_2H_2$ ranges from 0.15 to 3.80 mol%. $C_2H_4$ only occurs in two wells, with concentration of 0.17 mol% in Well T12 and 20.62 mol% in Q85. The concentration of $C_3H_6$ ranges from 0.17 to 6.00 mol%, $C_3H_8$ ranges from 0.52 to 6.46 mol%, $C_4H_6$ ranges from 1.10 to 2.30 mol%, and $C_6H_6$ ranges from 0.32 to 4.85 mol%.

$H_2S$, $SO_2$, CO, $H_2$, $N_2$ were detected but usually at less than 1 mol% except Well F4 and Well F29 ($H_2S$ of 4.00 mol% and 15.11 mol%, respectively) and the CO contents in Well F29 range from 1.38 mol% to 2.61 mol%. The concentrations of reductive gases such as CO and $H_2S$ are in negative relationship

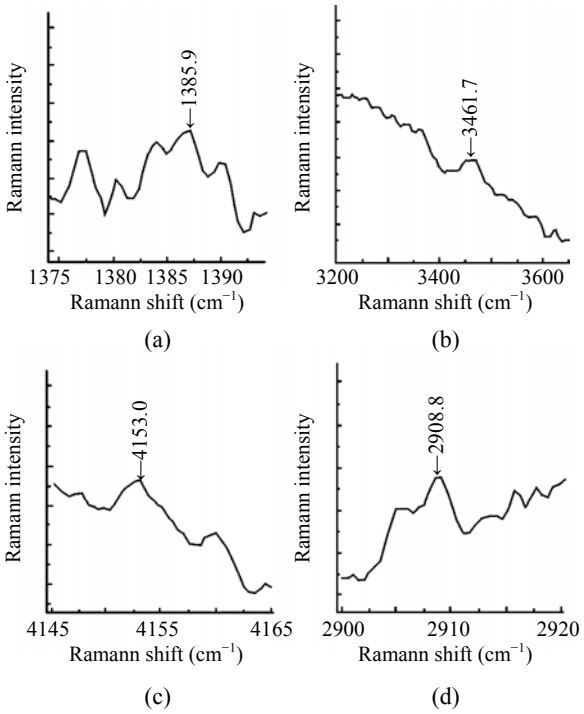


**Fig.3 Typical Raman spectra patterns of the detected gaseous compositions of the samples. (a) $CO_2$; (b) $H_2O$; (c) $H_2$; (d) $CH_4$**

**Table 2 The composition of the inclusions in Gangxi Fault Belt, Huanghua Depression**

| Well | Horizon | Depth (m) | Lithology | Components (mol%) | | | | | | | | | | | | | | |
|---|---|---|---|---|---|---|---|---|---|---|---|---|---|---|---|---|---|---|
| | | | | $CO_2$ | $H_2S$ | $SO_2$ | $H_2O$ | CO | $N_2$ | $H_2$ | $CH_4$ | $C_2H_2$ | $C_2H_4$ | $C_2H_6$ | $C_3H_6$ | $C_3H_8$ | $C_4H_6$ | $C_6h_6$ | Ratio* |
| F29 | $Es_1$ | 3014.29 | Sandstone | 0.00 | 15.11 | 0.00 | 71.51 | 0.00 | 0.00 | 0.52 | 4.18 | 0.00 | 0.00 | 0.00 | 1.33 | 4.37 | 0.00 | 2.99 | 0.66 |
| F14 | $Es_3$ | 3084.23 | Sandstone | 29.05 | 0.68 | 4.85 | 50.54 | 0.00 | 0.00 | 0.00 | 4.27 | 0.55 | 0.00 | 1.03 | 6.00 | 3.05 | 0.00 | 0.00 | 0.56 |
| S10 | $Es_3$ | 2343.46 | Sandstone | 22.80 | 0.00 | 0.00 | 62.61 | 0.00 | 0.00 | 0.00 | 4.23 | 3.76 | 0.00 | 0.00 | 1.62 | 0.00 | 0.00 | 0.00 | 0.44 |
| T16 | $Es_3$ | 3442.57 | Sandstone | 27.50 | 0.00 | 0.19 | 61.47 | 1.38 | 0.00 | 0.00 | 0.34 | 0.15 | 0.00 | 5.63 | 0.00 | 0.00 | 2.30 | 3.14 | 0.52 |
| Q85 | $Es_3$ | 3024.45 | Sandstone | 2.89 | 0.00 | 0.97 | 56.43 | 0.00 | 0.00 | 0.00 | 9.12 | 0.29 | 20.62 | 4.85 | 0.00 | 0.00 | 0.00 | 4.85 | 0.35 |
| T9 | O | 2996.27 | Carbonate | 18.66 | 0.44 | 0.00 | 66.22 | 2.16 | 0.00 | 0.00 | 0.47 | 0.00 | 0.00 | 5.80 | 4.00 | 2.27 | 0.00 | 0.00 | 0.68 |
| F4 | O | 2214.09 | Carbonate | 3.73 | 0.00 | 4.00 | 77.14 | 0.00 | 0.00 | 0.00 | 4.66 | 0.00 | 0.00 | 5.69 | 0.00 | 0.52 | 0.00 | 4.28 | 0.72 |
| T12 | O | 1980.00 | Carbonate | 35.49 | 0.32 | 4.18 | 42.47 | 2.54 | 0.00 | 0.14 | 8.35 | 0.00 | 0.17 | 0.00 | 0.00 | 6.46 | 0.00 | 0.00 | 0.99 |
| T13 | O | 2065.00 | Carbonate | 1.25 | 0.32 | 0.00 | 82.93 | 1.50 | 0.44 | 0.00 | 9.54 | 3.80 | 0.00 | 0.00 | 0.17 | 0.00 | 1.40 | 0.00 | 0.64 |
| T14 | O | 3043.00 | Carbonate | 10.29 | 0.28 | 0.00 | 76.86 | 2.61 | 0.49 | 0.00 | 6.58 | 1.52 | 0.00 | 1.33 | 0.00 | 0.00 | 1.10 | 0.00 | 0.75 |
| T15 | O | 2618.98 | Carbonate | 34.68 | 0.00 | 0.00 | 49.78 | 0.00 | 0.00 | 0.30 | 8.57 | 0.00 | 0.00 | 2.21 | 4.16 | 0.00 | 0.00 | 0.32 | 0.71 |

* ratio=($CH_4$+$C_2H_6$+$C_3H_8$)/organic components

with those of oxidative gases such as $SO_2$. For instance, in Well F29 the concentration of $H_2S$ is 15.11 mol%, while no $SO_2$ was detected. In Well F14 the condition is contrary, the concentration of $H_2S$ is only 0.68 mol%, while the $SO_2$ reaches to 4.85 mol%. If the fluids in the inclusion had formed under reducing conditions, the reductive gases such as CO or $H_2S$ would be dominating, vice versa.

**Occurrence of mantle-derived helium**

Helium is a trace constituent in natural gas and is the lightest element of all rare gases. Formed during natural nuclear processes, helium is chemically stable. Due to its strong diffusibility and permeability, helium can be used as a very sensitive tracer. Helium has two natural stable isotopes, $^3$He and $^4$He. $^3$He originates from the universal nebulae when the earth was formed, and $^4$He mainly originates from the radioactive disintegration of elements in the crust, such as U and Th (Wang, 1989). In particular, there is a factor of about 1000 times differences between the helium isotope ratios ($^3$He/$^4$He) of the upper mantle ($6R_a$~$9R_a$, where *Ra* is the atmosphere $^3$He/$^4$He ratio) and He produced in the crust ($0.01R_a$~$0.05R_a$) which allows He isotopes to provide a unique insight into processes where mantle volatiles are added to the continental crust (Stuart *et al*., 1995; Burnard *et al*., 1999; Allègre *et al*., 1995; Gautheron *et al*., 2005), i.e. if $R/R_a>1$, mantle-derived helium would be indicated, otherwise it is mainly crust-derived.

Table 3 shows that the $^3$He/$^4$He ratios ($R$) of the fluid inclusions from the Ordovician carbonates in the Gangxi Fault Belt range from $1.7\times10^{-6}$ to $3.44\times10^{-6}$, which are higher than the representative value of crust-derived one ($2.0\times10^{-8}$). The air-derived $^3$He/$^4$He ($R_a$) is $(1.40\pm0.03)\times10^{-6}$. The $R/R_a$ values range from 1.21 to 2.45 with an average of 1.83, which suggests the input of mantle-derived helium. The percent of the mantle-derived helium could be calculated using a mixing model of the mantle-derived helium ($^3$He/$^4$He$_{helium}$) and crust-derived helium ($^3$He/$^4$He$_{crust}$) by using the following formula (Burnard *et al*., 1999):

$$\text{Helium}_{mantle}\ (\%)=[(^3\text{He}/^4\text{He}_{sample}-^3\text{He}/^4\text{He}_{crust})/(^3\text{He}/^4\text{He}_{mantle}-^3\text{He}/^4\text{He}_{crust})]\times100\%,$$

where Helium$_{mantle}$, $^3$He/$^4$He$_{sample}$ and $^3$He/$^4$He$_{crust}$ represent the mantle-derived helium value, the helium value of sample and the crust-derived helium value, respectively. The end members of the mantle-derived helium value and the curst-derived helium value are assumed to be $1.15\times10^{-5}$ and $2\times10^{-8}$, respectively. The calculated results show that the percent of the contribution of the mantle-derived helium to the inclusions ranges from 14.63% (Well T13) to 29.74% (Well T15).

The $^3$He/$^4$He values of the fluid inclusions from the Shahejie Formation sandstones are in the range of $3.13\times10^{-7}$~$2.70\times10^{-6}$, which are also higher than the representative value of the crust-derived one. There-

**Table 3 Helium characteristics of the inclusions in Gangxi Fault Belt, Huanghua Depression**

| Well | Strata | Depth (m) | Lithology | $^3$He/$^4$He | $R/R_a$ | Helium$_{mantle}$ (%) |
|---|---|---|---|---|---|---|
| F14 | $Es_1$ | 3084.23 | Sandstone | $(1.84\pm0.08)\times10^{-6}$ | 1.32 | 15.85 |
| F29 | $Es_1$ | 3014.29 | Sandstone | $(9.54\pm0.37)\times10^{-7}$ | 0.68 | 0.68 |
| S10 | $Es_2$ | 2343.46 | Sandstone | $(3.13\pm0.25)\times10^{-7}$ | 0.22 | 2.55 |
| F15-1 | $Es_3$ | 3128.65 | Sandstone | $(8.25\pm0.44)\times10^{-7}$ | 0.59 | 7.01 |
| T16 | $Es_3$ | 3442.57 | Sandstone | $(1.11\pm0.06)\times10^{-6}$ | 0.79 | 9.49 |
| Q85 | $Es_3$ | 3024.45 | Sandstone | $(4.31\pm0.88)\times10^{-7}$ | 0.31 | 3.58 |
| F6 | $Es_3$ | 2467.00 | Carbonate | $(2.70\pm0.08)\times10^{-6}$ | 1.93 | 23.34 |
| F7 | Mz | 2314.00 | Carbonate | $(2.44\pm0.09)\times10^{-6}$ | 1.74 | 21.08 |
| T11 | Є | 2868.00 | Carbonate | $(1.51\pm0.05)\times10^{-6}$ | 1.08 | 12.98 |
| F4 | O | 2214.09 | Carbonate | $(2.09\pm0.06)\times10^{-6}$ | 1.49 | 18.03 |
| T9 | O | 2996.27 | Carbonate | $(2.94\pm0.08)\times10^{-6}$ | 2.10 | 25.44 |
| T12 | O | 1980.00 | Carbonate | $(3.19\pm0.08)\times10^{-6}$ | 2.28 | 27.61 |
| T13 | O | 2065.00 | Carbonate | $(1.70\pm0.05)\times10^{-6}$ | 1.21 | 14.63 |
| T14 | O | 3043.00 | Carbonate | $(2.08\pm0.07)\times10^{-6}$ | 1.48 | 17.94 |
| T15 | O | 2618.98 | Carbonate | $(3.44\pm0.09)\times10^{-6}$ | 2.45 | 29.74 |

fore the inclusions of the Oligocene Shahejie Formation sandstones also have the input of mantle-derived helium, although the $R/R_a$<1 of the Well F29, S10, F15, T16, Q85 means the helium is mainly crust-derived. Using the above-mentioned formula we calculated that the mantle-derived helium contributions range from 2.55% (Well S10) to 23.34% (Well F6).

We also analyzed two samples of the Cambrian carbonates and Mesozoic carbonates. The results also show the input of mantle-derived helium, with the contribution of 12.98% (Well T11) and 21.08% (Well F7), respectively.

## DISCUSSION

### Trapping time of the fluid flows

Recently, a few publications have been directed to the possibility of fluid inclusion's homogenization temperatures ($T_h$) to distinguish the individual fluid flow events and constrain the relative timing of flow migration, with combination of burial and geothermal history of the host rock (Karlsen *et al*., 1993; Xiao *et al*., 2002; Ding *et al*., 2005). The aqueous inclusions' homogenization temperature can represent their host rock temperature (Maurice and Jean-Bacques, 1997).

To determine the depth when the aqueous fluid inclusions formed, we applied the equation: $H=(T_h-T_0)/PGT$, where $H$ is the depth (m) at which the fluid inclusions formed; $T_h$ is the measured fluid inclusion homogenization temperature (°C), $T_0$ is the paleo-surface temperature (°C) and $PTG$ is the palaeogeothermal gradient (°C/100 m). The $PTG$ of the Shahejie Formation in the Gangxi Fault Belt is 3.4 °C/100 m (Tian *et al*., 2000), and 3.0 °C/100m for the Ordovician strata here (Zhu and Qin, 2001). $T_0$ is 20 °C. The calculating results show that the $H$ is 3110 m, 3476 m, 3841~4434 m and 4183~5183 m for the inclusions in the $Es_1$, $Es_2$, $Es_3$ and Ordovician strata, respectively. According to the buried-history curve we can determine that the trapping time for the fluid flows in the inclusions of the $Es_1$ member is in the Minghuazhen Period (Nm) of the Neocene (about 3 Ma), Nm for the $Es_2$ member (about 6 Ma), late Ng (Guantao Period)-Nm for the $Es_3$ member (14~6 Ma), and Ng-Nm for the Ordovician (20~3 Ma). So the helium input of the Shahejie Formation and Ordovician carbonates occurred in Neocene (Fig.4).

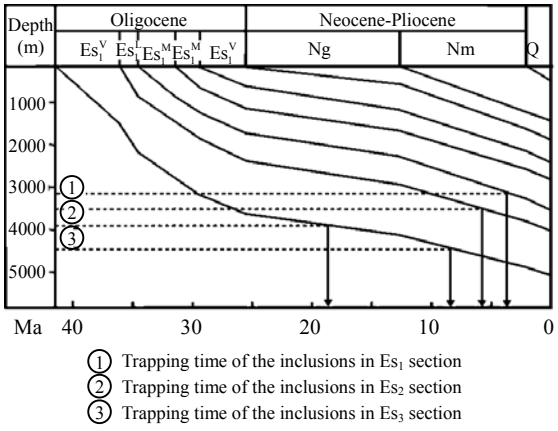


(a)

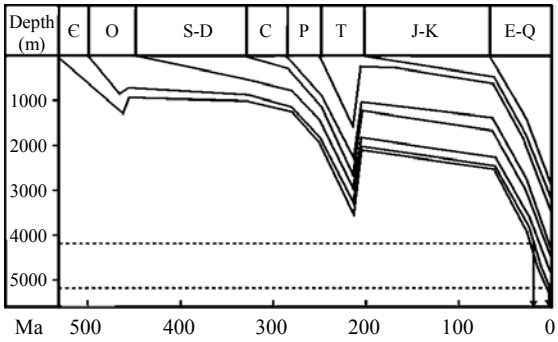


(b)

**Fig.4 Trapping time of the inclusions in Eocene-Oligocene Shahejie Formation (a) and Ordovician (b) (Both the buried-history curves are according to the Dagang Oilfield of CNPC)**

### Relationship between the mantle-derived helium and the faults

An isoline map of the mantle-derived helium was drawn (Fig.5). The fluid inclusions of the Ordovician carbonates and the Oligocene Shahejie Formation are in the same map of the mantle-derived helium occurring in Neocene. Fig.5 shows that the percentage of mantle-derived helium has close relationship with the two faults in this area: one is the Gangxi Fault trending NE, the other is the Xuzhuangzi Fault trending NWW. The $R/R_a$ values are generally high in the samples along the Gangxi Fault, indicating the high percentage of the mantle-derived helium. The highest percentage occurs in the intersectional area of the Gangxi and Xuzhuangzi faults. For instance, the $R/R_a$ value of Well T15 is 2.45, and that of Well T12 is 2.28. The $R/R_a$ values decrease from the intersection to the outside. Fig.6a shows the

$R/R_a$ values vertical to the Gangxi Fault. The value decreases from 1.93 of Well F6 in the intersectional area to 0.22 of the Well S10, and 0.31 of the well Q85. Fig.6b showing the $R/R_a$ values along the Gangxi Fault has the same characteristics, i.e. the value decreases from 2.45 of Well T15 to 1.48 of Well T14.

Two fundamental conditions are necessary for the upward invasion of mantle-derived helium: mantle uplift causing the movement of magma that carries mantle-originated gas, and the deep-rooted tension faults which provide the passages (Dai *et al*., 1995). The characteristics of helium isotopes in the Gangxi Fault Belt clearly show its relationship to the tectonic setting. The study area is located in the middle of the Bohai Bay Basin. Geologically the Bohai Bay Basin is an extensional basin developed in Cenozoic, and was mainly influenced by the movement of Pacific Plate. Since the late Cretaceous, the eastern Asia marginal subduction zone changed from andesite type (compressional) in the Mesozoic into arc-marginal sea type (extensional) in the Cenozoic. With the back arc extension and the mantle uplift, Bohai Bay Basin was in extensional stress field. Widespread NE-NEE direction rift systems and strong magma activities occurred (Ren *et al*., 2002).

Deep faults, as pathways for mantle magma, may provide favorable pathways for the migration of mantle-derived gases during extension. However, these NWW trending faults, such as the Xuzhuangzi fault, are strike-slip in Cenozoic and the openness condition is not good. Only when they are intersected by the NE trending extensional faults, such as the Gangxi Fault, could they become the favorable sites for the discharge of gases (Fig.7). The intersection of the Gangxi and Xuzhuangzi faults has the highest percentage of the mantle-derived helium, and the $R/R_a$ value reduces from the center to the surrounding areas.

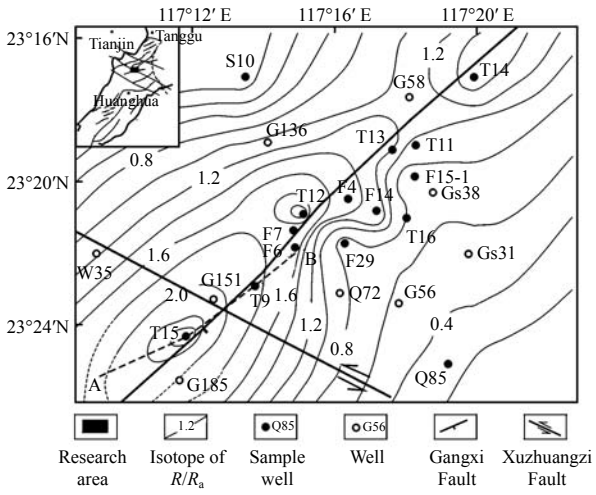


**Fig.5 $R/R_a$ isoline map in Gangxi Fault Belt**

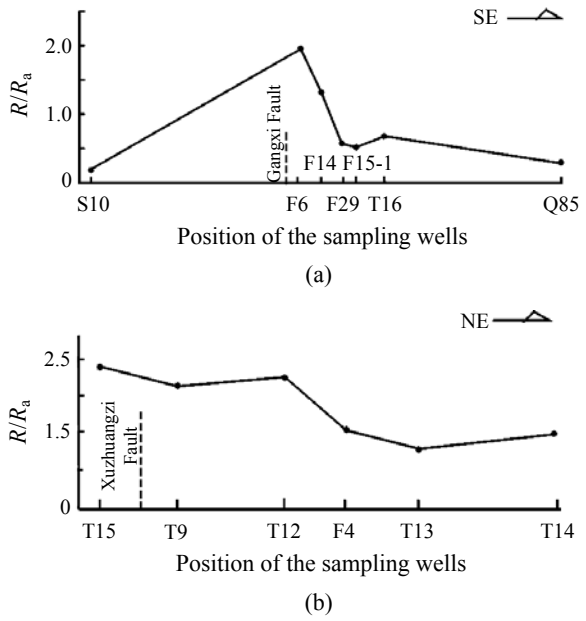


**Fig.6 The distribution of $R/R_a$ vertical to the Gangxi Fault (a) and along the Gangxi Fault (b)**

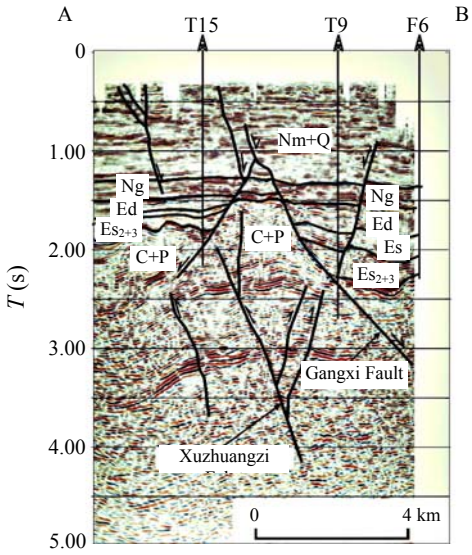


**Fig.7 Seismic profile across the Xuzhuangzi Fault. The position of the profile is shown in Fig.5**

**Relationship between the hydrocarbon maturity and the faults**

Since the 1950s many hydrocarbon evolution simulation experiments have been done to simulate the evolution of organic compositions and forming process of hydrocarbon under short-term and high-temperature condition (Hawkes, 1972; Saxby and Riley, 1984; Simoneit, 1990; Behar *et al*., 1992; Price and McNeil, 1997). The results show that the maturation process is a hydrogenation process during which the organic compositions turn into alkane. So we can use the concentration ratio between the normal alkane ($CH_4$, $C_2H_6$, $C_3H_8$) and the total organic compositions to represent the hydrocarbon maturity degree, i.e. the higher the ratio, the higher the maturity. The ratios are shown in Table 2 and Fig.8. The high values occur in the intersectional area of the Gangxi Fault and the Xuzhuangzi Fault. Vertically to the Gangxi Fault, the values have the same characteristics, i.e. the value decreases from 0.99 of Well T12 to 0.44 of Well S10, and 0.35 of the well Q85.

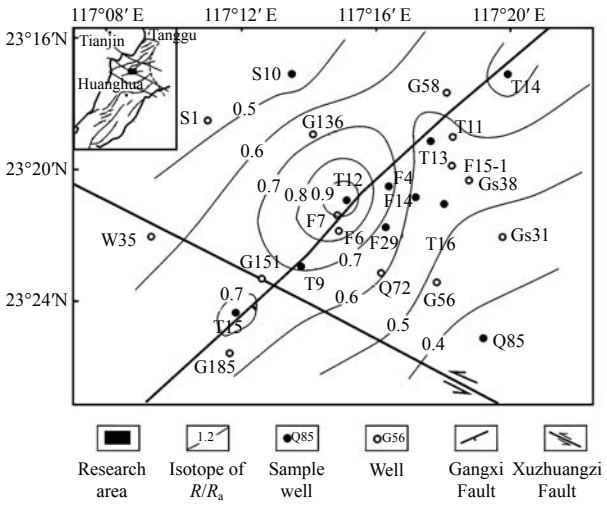


**Fig.8 The distribution of hydrocarbon maturity of fluid inclusion in the Gangxi Fault Belt**

The deep faults not only provide favorable pathways for the migration of mantle-derived gases during extension, they also might accord with high geothermal field. The highest geothermal gradient generally locates near the faults (Fig.9) as they favor the rise of deep heat flows (Stiros, 1995; Wang, 1984; Jonathan, 2004). High temperature is a key factor promoting the maturity of the hydrocarbon (Ismail and Shamsuddin, 1991; McCarty and Felbeck, 1986). That is why the wells with high hydrocarbon maturity locate in the intersection area of Gangxi Fault and the Xuzhuangzi Fault.

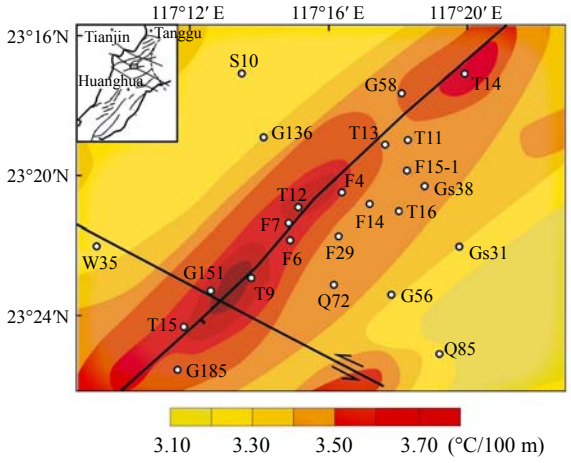


**Fig.9 Geothermal gradient in the Gangxi Fault Belt**

## CONCLUSION

(1) The fluid inclusions of the Ordovician carbonates and the Oligocene Shahejie Formation's sandstones in the Gangxi Fault Belt, Huanghua Depression, Bohai Bay Basin, are secondary with gas/liquid ratios of 5%~10% generally. $H_2O$ comprises the main composition, with $CO_2$ and $CH_4$ making up the remaining bulk. Studies on the homogenization temperatures, together with the burial and geothermal history of the host rock, show that the fluid flows in the Shahejie Formation and the Ordovician carbonates were trapped in Neocene.

(2) The mantle-derived helium occurred not only in the fluid inclusions of the Ordovician carbonates, but also in the Shahejie Formation. The percentage of mantle-derived helium in the fluid inclusions is controlled by the NE trending Gangxi Fault and NWW trending Xuzhuangzi Fault. Higher $R/R_a$ values indicate stronger activities of the mantle degassing.

(3) The fault activities in the study area not only favor the uplifting of mantle-derived gases, but can also increase the hydrocarbon maturity. Heat flows may migrate upward through faults and form high geothermal field. The high temperature can promote the hydrocarbon maturity.

ACKNOWLEDGEMENTS

We thank Xiao Dunqing and Zhang Weijiang, Dagang Oilfield of CNPC, for their help during the sampling, and Sun Mingliang, Key Laboratory of Gas-Geochemistry, Lanzhou Institute of Geology, Chinese Academy of Sciences, for his help in the sample analyses.

## References

Allègre, C., Moreira, M., Staudacher, T., 1995. $^{4}He/^{3}He$ dispersion and mantle convection. *Geophys. Res. Lett.*, **22**(17):2325-2328. [doi:10.1029/95GL02307]

Aplin, A.C., Macleod, G., Larter, S.R., Pedersen, K.S., Soenshen, H., Booth, T., 1999. Combined use of Confocal Laser Scanning Microsscopy and PVT simulation for estimating the composition and physical properties of petroleum in fluid inclusions. *Marine and Petroleum Geology*, **16**(2):97-110. [doi:10.1016/S0264-8172(98)00079-8]

Bach, W., Naumann, D., Erzinger, J., 1999. A helium, argon and nitrogen record of the upper continental crust (KTB drill holes, Oberpfalz, Germany): implications for crustal degassing. *Chemical Geology*, **160**(1-2):81-101. [doi:10.1016/S0009-2541(99)00058-3]

Behar, F., Kressmann, S., Rudkiewicz, J.L., 1992. Experimental simulation in a confined system and kinetics modelling of kerogen and oil cracking. *Organic Geochemistry*, **19**(1-3):173-189. [doi:10.1016/0146-6380(92)90035-V]

Burnard, P.G., Hu, R., Turner, G., Bi, X.W., 1999. Mantle, crustal and atmospheric noble gases in Ailaoshan Gold deposits, Yunan Province, China. *Geochimica et Cosmochimica Acta*, **63**(10):1595-1604. [doi:10.1016/S0016-7037(99)00108-8]

Cao, J., Yao, S.P., Jin, Z.J., Hu, W.X., Zhang, Y.J., Wang, X.L., Zhang, Y.Q., Tang, Y., 2006. Petroleum migration and mixing in the northwestern Junggar Basin (NW China): constraints from oil-bearing fluid inclusion analyses. *Organic Geochemistry*, **37**(7):827-846. [doi:10.1016/j.orggeochem.2006.02.003]

Dai, C.S., Dai, J.X., Yang, C.Y., 1994. Tectonogeochemical characteristics of inorganic gases in Gangxi Fault of Huanghua Depression. *Chinese Science Bulletin*, **39**(9):748-753.

Dai, J.X., Song, Y., Dai, C.S., Chen, A.F., Sun, M.L., Liao, Y.S., 1995. Conditions Governing the Formation of Abiogenic Gases and Gas Pools in Eastern China. Science Press, Beijing, p.71-77 (in Chinese).

Dallai, L., Magro, G., Perucci, E., Ruggieri, G., 2005. Stable isotope and noble gas isotope compositions of inclusion fluids from Larderello geothermal field (Italy): Constraints to fluid origin and mixing processes. *Journal of Volcanology and Geothermal Research*, **148**(1-2):152-164. [doi:10.1016/j.jvolgeores.2005.03.019]

Ding, W.W., Dai, J.X., Yang, C.Y., Tao, S.Z., Hou, L., 2005. Helium isotopic compositions in fluid inclusions of the Gangxi fault belt in the Huanghua Depression, Bohai Bay Basin. *Chinese Science Bulletin*, **50**(22):2621-2627. [doi:10.1360/982004-855]

Doğan, T., Sumino, H., Nagao, K., Notsu, K., 2006. Release of mantle helium from forearc region of the Southwest Japan arc. *Chemical Geology*, **233**(3-4):235-248. [doi:10.1016/j.chemgeo.2006.03.008]

ECPGDO (Editorial Committee of Petroleum Geology of Dagang Oilfield), 1991. Petroleum Geology of Dagang Field. Petroleum Industry Press, Beijing, p.74-95 (in Chinese).

England, W.A., Mackenzie, A.S., Mann, D.M., Quigley, T.M., 1987. The movement and entrapment of petroleum fluids in the subsurface. *Journal of the Geological Society London*, **144**:327-347.

Feely, M., Parnell, J., 2003. Fluid inclusion studies of well samples from the hydrocarbon prospective porcupine basin, offshore Ireland. *Journal of Geochemical Exploration*, **78-79**:55-59. [doi:10.1016/S0375-6742(03)00134-1]

Gautheron, C., Moreira, M., Allègre, C., 2005. He, Ne and Ar composition of the European lithospheric mantle. *Chemical Geology*, **217**(1-2):97-112. [doi:10.1016/j.chemgeo.2004.12.009]

Graupner, T., Niedermann, S., Kempe, U., Klemd, R., Bechtel, A., 2006. Origin of ore fluids in the Muruntau gold system: Constraints from noble gas, carbon isotope and halogen data. *Geochimica et Cosmochimica Acta*, **70**(21):5356-5370. [doi:10.1016/j.gca.2006.08.013]

Hawkes, H.E., 1972. Free hydrogen in genesis of petroleum. *AAPG Bull*, **56**(11):2268-2277.

Hoke, L., Poreda, R., Reay, A., 2000. The subcontinental mantle beneath southern New Zealand, characterized by helium isotopes in intraplate basalts and gas-rich springs. *Geochimica et Cosmochimica Acta*, **64**(14):2489-2507. [doi:10.1016/S0016-7037(00)00346-X]

Hu, R.Z., Burnard, P.G., Bi, X.W., 2004. Helium and argon isotope geochemistry of alkaline intrusion-associated gold and copper deposits along the Red River-Jingshajiang fault belt, SW China. *Chemical Geology*, **203**(3-4):305-317. [doi:10.1016/j.chemgeo.2003.10.006]

Ismail, M., Shamsuddin, A.H.M., 1991. Organic matter maturity and its relation to time, temperature and depth in the Bengal Foredeep, Bangladesh. *Journal of Southeast Asian Earth Sciences*, **5**(1-4):381-390. [doi:10.1016/0743-9547(91)90052-Y]

Jonathan, M.L., 2004. Scattering from a fault interface in the Coso geothermal field. *Journal of Volcanology and Geothermal Research*, **13**(1-2):61-75.

Karlsen, D.A., Nedkvitne, T., Larter, S.T., 1993. Hydrocarbon composition of authigenic inclusions: application to elucidation of petroleum reservoir filling history. *Geochimica et Cosmochimica Acta*, **57**(15):3641-3659. [doi:10.1016/0016-7037(93)90146-N]

Kendrick, M.A., Burgess, R., Pattrick, R.A., Turner, G., 2001. Fluid inclusion noble gas and halogen evidence on the origin of Cu-porphyry mineralizing fluids. *Geochimica et Cosmochimica Acta*, **65**(16):2651-2668. [doi:10.1016/S0016-7037(01)00618-4]

Maurice, P., Jean-Bacques, B., 1997. Thermal history constraints from studies of organic, clay minerals, fluid inclusions and apatite fission tracks at the ardeche paleo-margin. *Journal of Sedimentary Research*, **67**(1):235-240.

McCarty, H.B., Felbeck, G.T.Jr., 1986. High temperature simulation of petroleum formation—IV. Stable carbon isotope studies of gaseous hydrocarbons. *Organic Geochemistry*, **9**(4):183-192. [doi:10.1016/0146-6380(86)90068-9]

Moore, J.N., Norman, D.I., Kennedy, B.M., 2001. Fluid inclusion gas compositions from an active magmatic-hydrothermal system: a case study of the Geysers geothermal field, USA. *Chemical Geology*, **17**3(1-3):3-30. [doi:10.1016/S0009-2541(00)00265-5]

Muramatsu, Y., Sawaki, T., Arai, F., 2006. Geochemical study of fluid inclusions from the western upflow zone of the Matsukawa geothermal system, Japan. *Geothermics*, **35**(2):123-140. [doi:10.1016/j.geothermics.2006.01.003]

Oxburgh, E.R., O'Nions, R.K., 1987. Helium loss, tectonic and the terrestrial heat budget. *Science*, **237**(4822):1583-1588. [doi:10.1126/science.237.4822.1583]

Pang, L.S.K., George, S.C., Quezada, R.A., 1998. A study of the gross compositions of oil-bearing fluid inclusions using high performance liquid chromatography. *Organic Geochemistry*, **29**(5-7):1149-1161. [doi:10.1016/S0146-6380(98)00135-1]

Polyak, B.G., Prasolov, E.M., Cermak, V., 1985. Isotopic compositions of noble gases in geothermal fluids of the Krusne Hary Mts, Czechoslovakiy, and the nature of the local geothermal anomaly. *Geochimica et Cosmochimica Acta*, **49**(3):695-699. [doi:10.1016/0016-7037(85)90164-4]

Price, L.C., McNeil, R., 1997. Thoughts on the birth, evolution, and current state of petroleum geochemistry. *Journal of Petroleum Geology*, **20**:118-123.

Ren, J.Y., Kensaka, T., Li, S.T., 2002. Late Mesozoic and Cenozoic rifting and its dynamic setting in Eastern China and adjacent areas. *Tectonophysics*, **344**(3-4):175-205. [doi:10.1016/S0040-1951(01)00271-2]

Rocholl, A., Heusser, E., Kirsten, T., Oehm, J., Richter, H., 1996. A noble gas profile across a Hawaiian mantle xenolith: Coexisting accidental and cognate noble gases derived from the lithospheric and asthenospheric mantle beneath Oahu. *Geochimica et Cosmochimica Acta*, **60**(23):4773-4783. [doi:10.1016/S0016-7037(96)00273-6]

Saxby, J.D., Riley, K.W., 1984. Petroleum generation by laboratoryscale pyrolysis over six years simulating conditions in a subsiding basin. *Nature*, **308**(5955):177-179. [doi:10.1038/308177a0]

Simoneit, B.R.T., 1990. Petroleum generation, an easy and widespread process in hydrothermal system: An overview. *Applied Geochemistry*, **5**(1/2):17-28.

Stiros, S.C., 1995. The 1953 seismic surface fault: Implications for the modeling of the Sousake (Corinth area, Greece) geothermal field. *Journal of Geodynamics*, **20**(2):167-180. [doi:10.1016/0264-3707(94)00031-P]

Stuart, F.M., Burnard, P.G., Taylor, R.P., 1995. Resolving mantle and crustal contributions to ancient hydrothermal fluids: He-Ar isotopes in fluid inclusions from Dae Hwa W-Mo mineralisation, S. Korea. *Geochimica et Cosmochimica Acta*, **59**(22):4663-4673. [doi:10.1016/0016-7037(95)00300-2]

Sun, M.L., Chen, J.F., 1998. Study on the salt deposit crushing by the Vacuum-Electric-Magnetic-Breaker and measurement of noble gas isotope composition. *Acta Sedimentologica Sinica*, **16**(1):103-106 (in Chinese).

Tao, M.X., Xu, Y.C., Shen, P., 1997. Tectonic and geochemical characteristics and reserved conditions of a mantle source gas accumulation zone in Eastern China. *Science in China, Ser. D*, **40**(1):73-80.

Thiéry, R., Pironon, J., Walgenwitz, F., Montel, F., 2002. Individual characterization of petroleum fluid inclusions (composition and P-T trapping conditions) by microthermometry and confocal laser scanning microscopy: influences from applied thermodynamics of oils. *Marine and Petroleum Geology*, **19**(1):847-859. [doi:10.1016/S0264-8172(02)00110-1]

Tian, K.Q., Yu, Z.H., Feng, M., 2000. Paleogene Deep-Seated Hydrocarbon's Geology and Exploration in Bohai Bay Basin. Petroleum Industry Press, Beijing, p.121 (in Chinese).

Valbracht, P.J., Honda, M., Matsumoto, T., Mattielli, N., McDougall, I., Ragettli, R., Weis, D., 1996. Helium, neon and argon isotope systematics in Kerguelen ultramafic xenoliths: implications for mantle source signatures. *Earth and Planetary Science Letters*, **138**(1-4):29-38. [doi:10.1016/0012-821X(95)00226-3]

Wang, T.F., 1984. Recent tectonic stress field, active faults and geothermal fields (hot-water type) in China. *Journal of Volcanology and Geothermal Research*, **22**(3-4):287-289. [doi:10.1016/0377-0273(84)90006-4]

Wang, X.B., 1989. Geochemistry and Cosmochemistry of Rare Gas Isotope. Science Press, Beijing, p.7-22 (in Chinese).

Xiao, X.M., Liu, Z.F., Liu, D.H., Mi, J.K., Sheng, J.G., Song, Z.G., 2002. Determining natural gas accumulation period by fluid inclusions in reservoir. *Chinese Science Bulletin*, **47**(12):957-960.

Xu, Y.C., 1997. Helium isotope distribution of natural gases and its structural setting. *Earth Science Frontiers (China University of Geoscience, Beijing)*, **4**(3-4):185-190 (in Chinese).

Xu, Y.C., Shen, P., Liu, W.H., 1998. Noble Gas Geochemistry of Natural Gas. Science Press, Beijing, p.23-25 (in Chinese).

Zhu, Y.M., Qin, Y., 2001. Hydrocarbon-generation evolution of Paleozoic source rocks in the Konggu-3 well in Huanghua Depression. *Acta Petrolei Sinica*, **22**(6):30-33 (in Chinese).